

Article

Valorization of Biomass Through Anaerobic Digestion and Hydrothermal Carbonization: Integrated Process Flowsheet and Supply Chain Network Optimization

Sanja Potrč ^{1,*} , Aleksandra Petrovič ¹ , Jafaru M. Egieya ² and Lidija Čuček ^{1,*} 

¹ Faculty of Chemistry and Chemical Engineering, University of Maribor, Smetanova ulica 17, 2000 Maribor, Slovenia; aleksandra.petrovic@um.si

² Texas A&M Energy Institute, College Station, TX 77845, USA; jafaru.egieya@tamu.edu

* Correspondence: sanja.potrc@um.si (S.P.); lidija.cucek@um.si (L.Č.);
Tel.: +386-222-94-458 (S.P.); +386-222-94-452 (L.Č.)

Abstract: Utilization of biomass through anaerobic digestion and hydrothermal carbonization is crucial to maximize resource efficiency. At the same time, supply chain integration ensures sustainable feedstock management and minimizes environmental and logistical impacts, enabling a holistic approach to a circular bioeconomy. This study presents an integrated approach to simultaneously optimize the biomass supply chain network and process flowsheet, which includes anaerobic digestion, cogeneration, and hydrothermal carbonization. A three-layer supply chain network superstructure was hence developed to integrate the optimization of process variables with supply chain features such as transportation modes, feedstock supply, plant location, and demand location. A mixed-integer nonlinear programming model aimed at maximizing the economic performance of the system was formulated and applied to a case study of selected regions in Slovenia. The results show a great potential for the utilization of organic biomass with an annual after tax profit of 23.13 million USD per year, with the production of 245.70 GWh/yr of electricity, 298.83 GWh/yr of heat, and 185.08 kt/yr of hydrochar. The optimal configuration of the supply chain network, including the selection of supply zones, plant locations and demand locations, transportation links, and mode of transportation is presented, along with the optimal process variables within the plant.

Keywords: anaerobic digestion; hydrothermal carbonization; supply chain optimization; process flowsheet optimization; mathematical programming



Academic Editor: Alberto Maria Gambelli

Received: 15 December 2024

Revised: 2 January 2025

Accepted: 10 January 2025

Published: 14 January 2025

Citation: Potrč, S.; Petrovič, A.; Egieya, J.M.; Čuček, L. Valorization of Biomass Through Anaerobic Digestion and Hydrothermal Carbonization: Integrated Process Flowsheet and Supply Chain Network Optimization. *Energies* **2025**, *18*, 334. <https://doi.org/10.3390/en18020334>

Copyright: © 2025 by the authors. Licensee MDPI, Basel, Switzerland. This article is an open access article distributed under the terms and conditions of the Creative Commons Attribution (CC BY) license (<https://creativecommons.org/licenses/by/4.0/>).

1. Introduction

To adhere to the principles of a circular bioeconomy, address the challenges of waste management, reduce greenhouse gas emissions, and generate renewable energy sources [1,2], various methods can be used, from biological to chemical and thermal processes. In addition to conventional methods like anaerobic digestion (AD), advanced techniques such as hydrothermal carbonization (HTC) under subcritical or supercritical conditions and their combinations are gaining increasing attention.

AD is a promising method to produce biogas from waste biomass, whereby the digestate is formed as a by-product. Digestate is a nutrient-rich substance that can be used as a fertilizer or further processed through hydrothermal carbonization (HTC) to produce hydrochar, a stable, hydrophobic solid with similar fuel properties to lignite [3]. AD is a complex process that is influenced by various parameters that affect biogas production

and process stability. Key factors for optimizing the AD process include pH, temperature, organic loading rate, hydraulic retention time, and pressure [4]. Substrate characteristics, the inoculum-to-substrate ratio, and the carbon-to-nitrogen (C/N) ratio are crucial for anaerobic co-digestion (AcoD) [5]. Additionally, parameters such as volatile fatty acids, alkalinity, total solids, volatile solids, and potential inhibitors such as ammonia play an important role in the efficiency and stability of the AD process [6].

Alternatively, HTC converts biomass and organic waste into valuable products under moderate temperature and pressure conditions [7,8]. For instance, the HTC process can convert food waste [9], sewage sludge [10], green waste [2], and other sources into valuable products such as hydrochar and other biofuels such as bio-oil. It offers several advantages, including operating at lower temperatures than conventional thermal conversion methods [11] and the ability to process wet feedstocks to produce hydrochar [3], as well as higher efficiency, environmental safety, and economic benefits. The HTC process is influenced by various parameters such as temperature, residence time, water-to-biomass ratio, and feedstock composition [12]. HTC products are used in a variety of ways, including as a substitute for coal in power plants for energy generation, soil amendment, nutrient recovery [1], and carbon sequestration and adsorption for biogas purification [3].

HTC and AD are emerging technologies for sustainable waste management and resource recovery; therefore, their integration can bring about several benefits, such as improving energy recovery from biomass or waste, improving treatment efficiency, and reducing costs [9], as well as contributing to a circularity of materials [13]. When hydrochar is used as an additive in AD, it can significantly enhance biochemical reactions through various mechanisms. Hydrochar improves the solubilization and hydrolysis of organic matter, promotes the acidification of hydrolyzed products, and inhibits methanogenic bacteria while promoting key enzyme activities [14]. In addition, hydrochar provides attachment sites for microbial growth and contains surface functional groups that facilitate direct interspecies electron transfer (DIET), resulting in increased methane yield [15]. The addition of hydrochar in AD systems can also improve microbial species richness and uniformity, further contributing to the efficiency and stability of the process [15]. Several other mutual benefits have been identified, e.g., HTC of digestate can contribute to the increased carbon content and improve the ignition properties of hydrochar [16]. However, further research is needed to optimize these methods and processes, as well as to perform techno-economic analyses to ensure their commercial viability and widespread adoption [10].

The modeling and optimization of AD have been studied extensively using various approaches. Process simulation software such as Aspen Plus, BioWin, Aquasim, Simba, and others are commonly used for AD modeling [5]. Mathematical models range from comprehensive white box models to simplified black box models, with recent advances in machine learning techniques [17]. Nature-inspired techniques such as genetic algorithms and particle swarm optimization offer advantages in parallel computation and dynamic behavior for AD modeling [18], helping to predict biogas yield, optimize process parameters, and provide insights into system stability [19]. Various AD process simulation models have been developed using Aspen Plus software to predict biogas production from various substrates. These models consider the main stages of AD, including hydrolysis, acidogenesis, acetogenesis, and methanogenesis, with numerous reactions and kinetics [20]. The simulation models take into account factors such as inhibition, pH, temperature, and retention time [21], wherein validation using industrial and laboratory data has shown good agreement between simulated and experimental results. Sensitivity analyses were performed to investigate the effects of the different parameters on biogas production and composition [22].

On the other hand, several simulation and optimization models have also been used for HTC, involving kinetic, thermodynamic, and statistical approaches [23], as well as process, reactor, and plant modeling [24]. However, the current models face several limitations due to the complexity of the HTC reactions and feedstock characteristics. To advance HTC modeling, Ubene et al. [25] recommend focusing on six key areas: variable feedstock compositions, exothermic reaction heat, reactor type, scale-up, pre-pressurization, the heat up period, and feedstock porosity. A continuous HTC process model using the UniSim Design process simulator showed improved hydrochar characteristics compared to batch processes, particularly for biomass with a high cellulose content [26]. Aspen Plus software was used to develop process models for converting municipal solid waste to hydrochar via the HTC process and for the hydrothermal liquefaction (HTL) of biomass [27]. Additionally, other mathematical approaches such as empirical models, response surface methodology, kinetic models, and machine learning have been applied to HTL optimization [28].

Recent studies have explored the integration of HTC with AD to improve biomass waste management and energy recovery. For example, Aragón-Briceño et al. [29] investigated the integration of AD and HTC of sewage sludge and showed that this combination can increase net energy production by up to 10 times compared to AD alone. The integration of both processes also enables the treatment of process water from HTC, which has a high chemical oxygen demand, by AD to produce methane-rich biogas [11]. Another study investigated the optimization of the total energy yield from sewage sludge and pine sawdust using a coupled HTC-AD process, where the optimal operating parameters were determined using response surface methodology [30]. Technoeconomic and life cycle assessments have shown that this integrated approach can reduce the environmental impacts compared to AD alone, mainly due to the production of hydrochar as a potential substitute for fossil fuels, but on the other hand, increases the cost by 42% compared to conventional AD [31].

While the integration of AD and HTC processes is crucial for improving the energy recovery of biomass, the inclusion of the supply chain is equally important for holistic system optimization. Supply chain efficiency affects transportation costs, logistics, and the overall sustainability of the system. By optimizing the supply chain, it is possible to minimize transportation routes, reduce costs, ensure a reliable flow of raw materials, and incorporate the strategic optimization of resources [32]. The current research lacks studies that integrate the simultaneous optimization of supply chain networks and production processes, especially focusing on the valorization of residues through AD and HTC. To fill this research gap, this study aims to develop and demonstrate a comprehensive approach and methodology for the simultaneous optimization of the coupled AD-HTC process flowsheet and biomass supply chain network. Specifically, the goal is to create a mixed-integer nonlinear programming (MINLP) model that maximizes the economic performance of the holistic system while accounting for the various waste sources available in the region and their logistics.

2. Methodology for the Simultaneous Optimization of the Biomass Supply Chain Network and the AD-HTC Process Flowsheet

The methodology consists of an integrated approach in which the biomass supply network and the process flowsheet combining AD and HTC processes are integrated and optimized simultaneously. First, the integrated approach is presented, followed by the methodology and the demonstration case study.

2.1. Simultaneous Optimization of Supply Chain Network and AD-HTC Process Flowsheet

The study integrates supply chain network optimization and process flowsheet optimization into a comprehensive framework. The supply chain network consists of three layers (L1–L3), as shown in Figures 1 and 2. The first layer represents the availability and location of feedstocks $pb \in PB$ in each supply zone i (i_1-i_{22}), the second layer represents the AD-HTC processing facilities at potential locations n (n_1-n_5), and the third layer represents the demand for the products $prd \in PRD$ at locations j (j_1-j_{22}). Feedstocks available in each supply zone i could be transported to the AD-HTC plant at any potential location n . The products from each AD-HTC plant n could then be distributed to the demand locations j . Figure 1 shows the three-layer supply network superstructure and illustrates how the feedstocks pb from zone i_1 could be transported to each plant location n and how the products prd from n_1 could be distributed to each demand location j . The possible connections between other supply zones i and plant locations n , as well as possible connections between other plant locations n and end users j , were considered in the same way.

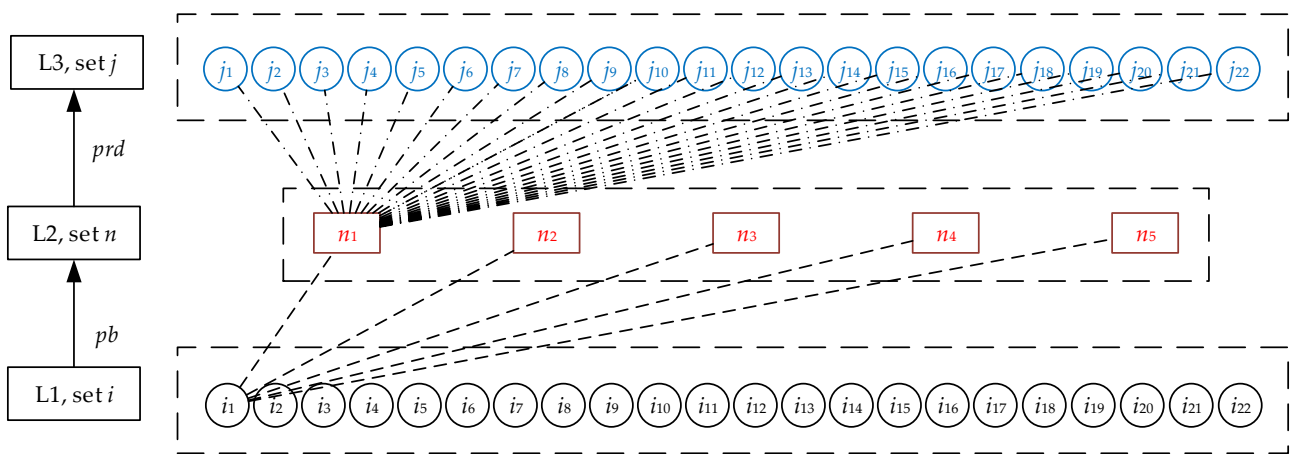


Figure 1. Three-layer supply network superstructure.

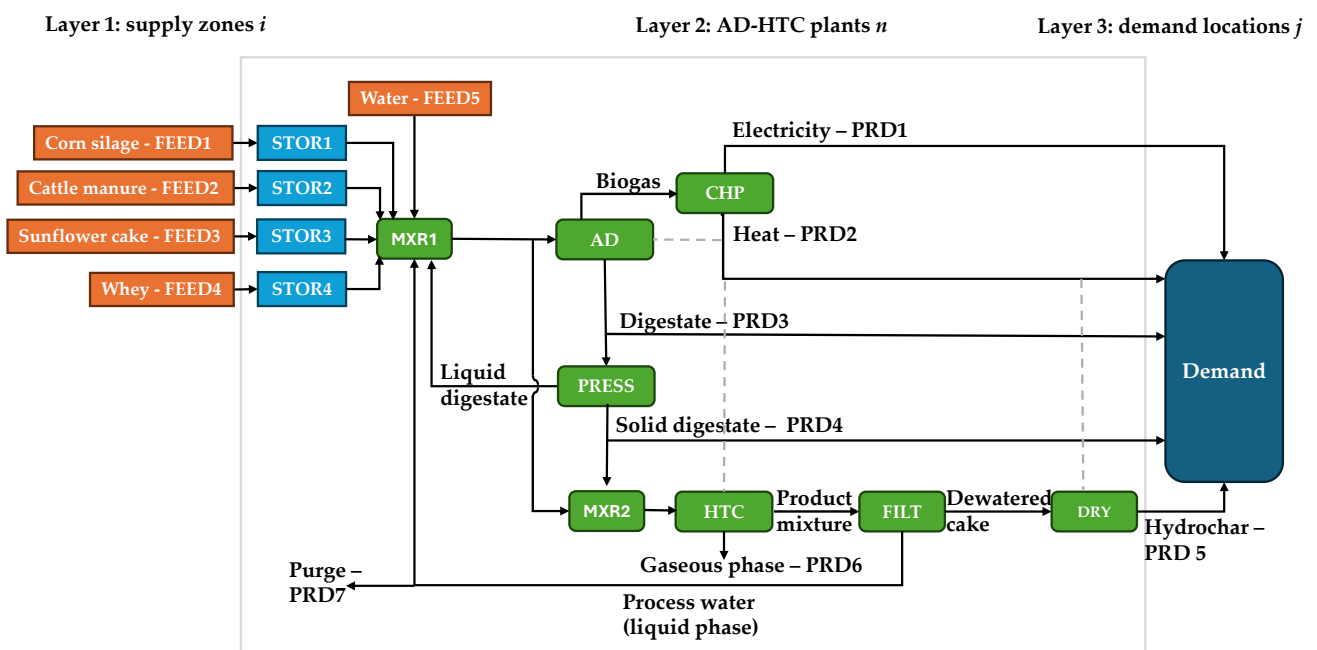


Figure 2. Schematic representation of the integrated supply network and AD-HTC process flowsheet optimization.

Figure 2 shows the schematic representation of the simultaneous optimization of the biomass supply chain network and the process flowsheet, which includes both AD and HTC processes, as well as combined heat and power (CHP) generation. The substrates considered in this case study were corn silage, cattle manure, sunflower cake, and whey due to their availability in the region and their suitable properties for AD and HTC processes. The feedstocks from supply zones i (Layer 1) could then be transported to the storage facilities at the plant sites n (Layer 2). From the storage facilities, they could be used for either AD or HTC. The biogas produced from the AD process is then used in combined heat and power (CHP) plants where electricity and heat are generated. The digestate obtained from the AD process can be used directly at the points of use or sent to the filter press (PRESS), where a solid and a liquid fraction are obtained. The liquid digestate can be used as a feedstock for AD or HTC, while the solid digestate can be used at demand sites or as a feedstock for the HTC process. The HTC process consists of a reactor, followed by a filtration (FILT) and drying (DRY) unit in which hydrochar is obtained as the main product, while process water and gaseous products are by-products. The process water can further be reused within the process. The main products ($prd \in PRD$), i.e., electricity, heat, digestate, solid digestate, and hydrochar, can then be distributed to the end users at demand locations j (Layer 3).

The following data were considered for the potential supply zones ($i \in I$):

- set of raw materials ($pb \in PB$), including corn silage, cattle manure, sunflower cake, and whey;
- land area of each supply zone i and the share of the actual area that could be used for growing crops;
- availability of raw materials pb in each zone i ;
- dry matter content, density, and moisture content of raw materials;
- biogas yield and methane content obtained from each raw material;
- cost of the raw materials.

For potential AD-HTC plants ($n \in N$), the following data were considered:

- yield of the conversion of raw materials to intermediate products, by-products, and main products;
- minimum and maximum plant capacities, energy consumption, and plant lifetime;
- fixed and variable storage costs of raw materials, the maximum period of storage;
- labor costs (fixed and variable);
- losses during storage and operation.

The following data were taken into account for the end users ($j \in J$):

- set of the products ($prd \in PRD$), including electricity, heat, digestate, and hydrochar;
- price of the products;
- demand locations.

Between the layers, different available transportation modes ($tro \in TRO$) were considered, such as road transport, pipelines, and transmission lines. Road transportation and pipelines were considered for the distribution of cattle manure and whey from the supply zones to storage at the plant site, while only road transportation was considered for corn silage and sunflower cake.

Pipelines were considered for heat distribution, power transmission lines for electricity, and road transportation for hydrochar, while two options were considered for digestate: pipeline or road transportation by truck. For road transportation, round trips were also considered, with a return trip factor of 2 [33].

The data for transportation from L1 to L2 and L2 to L3 are as follows:

- fixed and variable transportation costs of pb via different modes of transport from supply location i to plant site n ;
- fixed and variable transportation costs for the product prd from the plant location n to the final consumer j via the available transportation modes;
- losses during transportation.

Fixed transportation costs are associated with material handling, e.g., loading and unloading, while variable transportation costs depend on distances [34]. The above data are listed in Part A of the Supplementary Materials.

2.2. Mathematical Formulation

The problem of simultaneous optimization of the AD-HTC process flowsheet and supply chain network was formulated as a MINLP model. A three-layer supply network superstructure was considered, in which 22 supply locations $i \in I$ at L1, 5 plant sites $n \in N$ at L2, and 22 demand locations $j \in J$ at L3 could potentially be selected. The following sets and subsets were considered for the AD-HTC process flowsheet optimization:

- process units $u \in U$,

$$U = \left\{ \begin{array}{l} \text{FEED1, FEED2, FEED3, FEED4, FEED5,} \\ \text{STOR1, STOR2, STOR3, STOR4, MXR1, MXR2,} \\ \text{FSPL1, AD, CHP, ESPL, PRESS, FSPL2, FSPL3,} \\ \text{FSPL4, HTC, FILT, DRY, PRD1, PRD2, PRD3,} \\ \text{PRD4, PRD5, PRD6, PRD7} \end{array} \right\}$$

- raw materials feed $feed \in FEED, FEED \subset U$,

$$FEED = \{\text{FEED1, FEED2, FEED3, FEED4, FEED5}\}$$

- storages $stor \in STOR, STOR \subset U$,

$$STOR = \{\text{STOR1, STOR2, STOR3, STOR4}\}$$

- mixers $mxr \in MXR, MXR \subset U$,

$$MXR = \{\text{MXR1, MXR2}\}$$

- flow splitters $fspl \in FSPL, FSPL \subset U$,

$$FSPL = \{\text{FSPL1, FSPL2, FSPL3, FSPL4}\}$$

- products $prd \in PRD, PRD \subset U$,

$$PRD = \{\text{PRD1, PRD2, PRD3, PRD4, PRD5, PRD6, PRD7}\}$$

- all components $p \in P$,

$$P = \left\{ \begin{array}{l} \text{whey, silage, sunflower cake, cattle manure, H}_2\text{O, biogas,} \\ \text{digestate, liquid digestate, solid digestate, electricity, heat,} \\ \text{gaseous phase, product mixture, dewatered cake,} \\ \text{process water, hydrochar, purge, carbon, CH}_4, \\ \text{CO}_2, \text{ coal, natural gas, wood} \end{array} \right\}$$

- input and output flows for process units $io \in IO$,

$$IO = \{\text{in-1, in-2, in-3, in-4, in-5, in-6, in-7, out-1, out-2}\}$$

The subset $IN \subset IO$ included the elements in-1 to in-7 defined for the inlets and the subset $OUT \subset IO$ included the elements out-1 and out-2 for the outlets. The binary variables are used to determine the locations of the plants and to select the transportation modes and routes as follows:

- $yT_{u,n}$ for the existence of a process unit $u \in U$ at the potential location $n \in N$;
- $yL1L2_{i,n,pb,tro}$ to optimally select the route of the feedstocks $pb \in PB$ from the supply zone $i \in I$ to the plant location $n \in N$ via the transportation mode $tro \in TRO$;
- $yL2L3_{n,j,prd,tro}$ to optimally select the route of the products $prd \in PRD$ from the plant location $n \in N$ to the demand location $j \in J$ via the mode of transportation $tro \in TRO$.

Continuous variables to be optimized were the total mass flow rates within the supply chain, the mass flow rates of the components, the dry matter content and water content in each flow, the energy flows, the revenues, all costs, etc. The equality and inequality constraints, as well as the objective function, are presented in the following subsections.

2.2.1. Constraints

At layer 1, the availability of feedstocks $pb \in PB$ in each supply zone $i \in I$ must be determined. For this purpose, data on the total area of each zone (A_i^{TOTAL}) and the share of the total area in each zone $i \in I$ devoted to the cultivation of corn silage and sunflowers ($x_{i,pb}$) [35], as well as data on hectare yields ($HY_{i,pb}$) in $t/(km^2 \cdot y)$, were taken from the Statistical Office of the Republic of Slovenia [36]. The quantity of corn silage and sunflowers in each supply zone i in kt per year (kt/yr) therefore corresponds to the mass flow ($F_{i,n,pb}$) calculated using Equation (1).

$$\sum_n F_{i,n,pb} = HY_{i,pb} \cdot A_i^{\text{TOTAL}} \cdot x_{i,pb}, \forall i \in I, pb \in PB \quad (1)$$

To obtain the availability of sunflower cake in each zone, the mass flow of sunflowers was multiplied by the yield of sunflower cake from sunflowers. The amount of cattle manure in each zone was calculated as the number of cattle based on their age in each zone [37] multiplied by the amount of cattle manure produced per year by one cattle based on their age. To calculate the hectare yield of cattle manure required in Equation (1) (in $t/(km^2 \cdot y)$), the total amount of cattle manure was divided by the total area of each zone. Further details on the calculation of manure yield can be found in the Supplementary Material of the previous study by the authors [33]. For whey, the production in t/yr was taken from [38] and further divided by the total area of each zone to obtain the hectare yields required in Equation (1).

The link between L1 and L2 is established by integrating the feedstock pb from zone i at L1 and the units $feed \in FEED$ in the process flowsheet. As shown in Figure 1, corn silage is an output of unit FEED1, cattle manure is an output of FEED2, sunflower cake of FEED3, and whey of FEED4. For the integration, the new set $PBFEED \subseteq PB \times FEED$ was defined, which indicates the flow rate of each feedstock pb to the specified unit ($feed$) in the flowsheet. The total mass flow of feedstock pb transported from supply zone i to plant site n is defined by Equation (2):

$$\sum_{i \in I} F_{i,n,pb} = \sum_{feed \in FEED \wedge (pb, feed) \in PBFEED} F_{n,feed,pb}^{\text{out-1}}, \forall n \in N, pb \in PB \quad (2)$$

where $F_{i,n,pb}$ denotes the mass flow rate of feedstock pb from the supply zone i to the plant site n , and $F_{n,feed,pb}^{out-1}$ represents the outlet of pb from the unit $feed$ at location n .

At L2, the feedstock pb can be stored in the process unit $stor \in STOR$ in the AD-HTC plant n , with each $stor$ being intended for a different feedstock. Equality conditions for the total flow rate, component flow rate, dry matter content, and water flow rate were defined for the storage facility and all other process units $u \in U$ to guarantee the mass balance.

The feedstocks are then mixed. The mass balance for the mixer is described by Equation (3). For the MXR1 unit, seven inlet streams are considered (four inlets are from storage units representing the individual feedstock pb , water, liquid digestate, and process water), and the output is the joint stream with a mass flow rate $F_{n,mxr}^{out-1}$. The feedstock mass flow rates and the output mass flow rate are variables that are optimized according to the other constraints included in the model to ensure realistic and feasible operation.

$$\sum_{in \in IN} F_{n,mxr}^{in} = F_{n,mxr}^{out-1}, \forall n \in N, mxr \in MXR \quad (3)$$

This joint stream is then split into 2 streams in the process unit FSPL1, as shown in Equation (4), one of which is sent to the AD unit and the other to the HTC unit.

$$F_{n,fspl}^{out} = x_{n,fspl}^{out} \cdot F_{n,fspl}^{in-1}, \forall n \in N, out \in OUT, fspl \in FSPL \quad (4)$$

$F_{n,fspl}^{out}$ denotes the mass flow rate of each output out from $fspl$ at location n , $x_{n,fspl}^{out}$ is the split fraction of each output out at location n , and $F_{n,fspl}^{in-1}$ represents the mass flow rate into the $fspl$ at location n . It should be noted that the split fraction was defined as a positive variable so that it was possible to optimize how much of the feed is used for AD and how much for HTC. The sum of the two split fractions should be equal to 1.

The total mass flow rate in the process unit $ad \in AD$ at location n is multiplied by the corresponding conversion factor (m^3/t) to obtain the volume of biogas produced at location n ($F_{n,ad,biogas}^{out-1}$), as shown in Equation (5).

$$F_{n,ad,biogas}^{out-1} = \sum_{pad \in PAD} F_{n,ad,pad}^{in-1} \cdot f_{pad}^{convAD}, \forall n \in N, ad \in AD \quad (5)$$

The subset $pad \in PAD \subset P$ represents all feedstocks available for AD (including all pb , liquid digestate, and process water).

The amount of digestate produced in the digester at location n ($F_{n,ad,digestate}^{out-2}$) was calculated using Equation (6) as the difference between the mass flow rate of feedstocks into the digester and the mass of material contained in the biogas ($F_{n,ad,biogas}^{out-1} \cdot \rho_{biogas}$), where ρ_{biogas} is the density of the biogas.

$$F_{n,ad,digestate}^{out-2} = \sum_{pad \in PAD} F_{n,ad,pad}^{in-1} - F_{n,ad,biogas}^{out-1} \cdot \rho_{biogas}, \forall n \in N, ad \in AD \quad (6)$$

Lower and upper bounds on dry matter content of 2% to 15% are employed for the anaerobic digester (and for the digestate), as illustrated in Equations (7) and (8).

$$F_{dm,n,ad}^{in-1} \geq 0.02 \cdot (F_{dm,n,ad}^{in-1} + F_{water,n,ad}^{in-1}), \forall n \in N, ad \in AD \quad (7)$$

$$F_{dm,n,ad}^{in-1} \leq 0.15 \cdot (F_{dm,n,ad}^{in-1} + F_{water,n,ad}^{in-1}), \forall n \in N, ad \in AD \quad (8)$$

$F_{dm,n,ad}^{in-1}$ stands for the dry matter content, and $F_{water,n,ad}^{in-1}$ represents the amount of water in the anaerobic digester ad at location n .

The volume of methane produced (F_{n,ad,CH_4}^{out-1}) at location n was calculated using Equation (9):

$$F_{n,ad,CH_4}^{out-1} = \sum_{pad \in PAD} F_{n,ad,pad}^{in-1} \cdot f_{pad}^{convAD} \cdot x_{CH_4,pad}, \forall n \in N, ad \in AD \quad (9)$$

where $x_{CH_4,pad}$ is the proportion of methane in the biogas produced from the material pad . The energy content of the biogas was determined as the product of the amount of methane, the lower calorific value, and the density of CH_4 , as shown in Equation (10).

$$Q_{f,n,ad}^{out-1} = F_{n,ad,CH_4}^{out-1} \cdot LHV_{CH_4} \cdot \rho_{CH_4}, \forall n \in N, ad \in AD \quad (10)$$

Biogas is then led to the CHP unit, where it is converted into electricity and heat using the corresponding conversion factors. Both products can then be used either at the demand locations or as a resource for other process units within the flowsheet. The electricity and heat requirements for the AD plant were determined based on the conversion factors for heat and electricity consumption, expressed in GWh per Mm^3 of biogas produced.

The digestate obtained is divided into 2 streams in the FSPL2 process unit, as defined in Equation (4), with one stream being fed to the belt filter press (PRESS; digestate dewatering) and the other to the demand locations. In the PRESS process unit, the solid and liquid fractions of the digestate are obtained, with the dry matter content in the solid fraction being between 20 and 30% [39]. In this study, a dry matter content of 25% was assumed in the solid digestate. The amount of dry matter in the solid digestate ($F_{dm,n,press,solid_frac}^{out-1}$) was determined using Equation (11) and calculated as the difference between the mass flow rate of the digestate and the mass flow rate of the recycle (liquid digestate) divided by the dry matter content of the solid digestate.

$$F_{dm,n,press,solid_frac}^{out-1} = \frac{F_{n,press,digestate}^{in-1} - F_{n,press,liquid_frac}^{out-2}}{0.25}, \forall n \in N, press \in PRESS \quad (11)$$

The liquid digestate is then fed into the MXR1 and could be reused as a feedstock for AD or HTC, while the solid digestate could either be fed to the demand or used as a feedstock for the HTC process. Again, the proportion of solid digestate used for one of the options is the variable, so the more economically advantageous solution is achieved through optimization. The HTC process is represented by 3 process units: the reactor HTC, the filtration unit FILT, and the drying unit DRY. The output of the reactor is a product mixture that contains a solid and a liquid phase, whereby gaseous products are also produced, mainly containing CO_2 and, in smaller quantities, other gasses such as CO , H_2 , CH_4 , and light hydrocarbons [40]. The product mixture is then separated by filtration, where solid hydrochar and the liquid phase (process water) are obtained. After filtration, the hydrochar still contains a significant amount of moisture. A drying unit is used to further reduce the moisture content and obtain the hydrochar with the right properties. The hydrochar obtained could be used as a solid biofuel, soil amendment, adsorbent, etc. at the demand locations. The liquid phase is reused in the process, as shown in Figure 1.

The gaseous products were assumed to account for between 5 and 10% of the mass flow rate into the HTC process unit [25], as shown in Equations (12) and (13).

$$F_{n,htc,gaseous_p}^{out-2} \geq 0.05 \cdot \sum_{phtc \in PHTC} F_{n,htc,phtc}^{in-1}, \forall n \in N, htc \in HTC \quad (12)$$

$$F_{n,htc,gaseous_p}^{out-2} \leq 0.10 \cdot \sum_{phtc \in PHTC} F_{n,htc,phtc}^{in-1}, \forall n \in N, htc \in HTC \quad (13)$$

The subset $phtc \in PHTC \subset P$ represents all feedstocks available for the HTC process (including all pb , liquid digestate, solid digestate, and process water).

The remaining flow rate represents the product mixture (out-1 of HTC), which contains a liquid and a solid phase and is fed to the filtration unit. For the filtration unit FILT at location n , it was assumed that between 70 and 80% of the dry matter content in the input ($F_{dm,n,filt}^{in-1}$) should be converted into a dewatered cake (hydrochar), as shown in Equations (14) and (15), where $F_{dm,n,filt,dewatered_cake}^{out-1}$ represents the dry matter content in the dewatered cake after filtration in the process unit $filt$ at location n .

$$F_{dm,n,filt,dewatered_cake}^{out-1} \geq 0.70 \cdot F_{dm,n,filt}^{in-1}, \forall n \in N, filt \in FILT \quad (14)$$

$$F_{dm,n,filt,dewatered_cake}^{out-1} \leq 0.80 \cdot F_{dm,n,filt}^{in-1}, \forall n \in N, filt \in FILT \quad (15)$$

Output 2 from the filtration unit, which represents the liquid phase, can either be reused in the process or discharged. For this purpose, the process unit FSPL4 was used and modeled, as shown in Equation (4), for FSPL1. For the drying unit, it was assumed that hydrochar with a dry matter content between 80% and 90% is obtained, as shown in Equations (16) and (17), where $F_{dm,n,dry,hydrochar}^{out-1}$ is the dry matter content of the hydrochar, and $F_{n,dry,hydrochar}^{out-1}$ is the total mass flow rate of the hydrochar.

$$F_{dm,n,dry,hydrochar}^{out-1} \geq 0.80 \cdot F_{n,dry,hydrochar}^{out-1}, \forall n \in N, dry \in DRY \quad (16)$$

$$F_{dm,n,dry,hydrochar}^{out-1} \leq 0.90 \cdot F_{n,dry,hydrochar}^{out-1}, \forall n \in N, dry \in DRY \quad (17)$$

The connection between L2 and L3 is established by integrating the products prd from the zones n at L2 and the products available for supply ($sprd \in SPRD$). For the integration, the new set $PRDSPRD \subseteq PRD \times SPRD$ was defined, which specifies the flow of each product prd to the specified product $sprd$ in the next supply chain layer L3. Electricity is an input for SPRD1, heat is an input for SPRD2, digestate for SPRD3, solid digestate for SPRD4, and hydrochar for SPRD5. It is assumed that the end consumers at demand location j can accept the products from multiple plants n . The total flow of the product prd transported from the plant location n to the demand location j is defined by Equation (18):

$$\sum_{j \in J} F_{n,j,prd} = \sum_{sprd \in SPRD \wedge (prd,sprd) \in PRDSPRD} F_{n,sprd,prd}^{in-1}, \forall n \in N, prd \in PRD \quad (18)$$

where $F_{n,j,prd}$ denotes the mass flow rate of the product prd from the plant location n to the demand location j , and $F_{n,sprd,prd}^{in-1}$ represents the inlet of prd into $sprd$.

2.2.2. Objective Function

The objective function of the integrated supply chain network and the AD-HTC process flowsheet optimization problem is to maximize the annual profit after tax (P_A), which is defined as the profit before tax (P_B) reduced by tax expenses ($P_B \cdot r_t$), as shown in Equation (19):

$$P_A = (1 - r_t) \cdot P_B \quad (19)$$

where r_t denotes the tax rate. Profit before tax is further defined as the revenue (R_{total}) reduced by the total costs (C_{total}), as shown in Equation (20). The revenue in millions of dollars per year (M\$/yr) is obtained from the sale of electricity, heat, digestate (dry or wet fraction), and hydrochar ($sprd$) from L2 (plant location n) to L3 (demand location j). The total costs in M\$ per year are the sum of the costs for the feedstocks pb transported from i to n and the additional purchase of raw materials at plant site n , the transportation costs

between the layers (TC), the storage costs (SC), the labor costs (LC), the discounted capital costs (DCC), the maintenance costs (MC), the other miscellaneous costs (OMC), and the other costs (OC).

$$P_B = R_{total} - C_{total} = \sum_{prd \in PRD} \sum_{n \in N} \sum_{j \in J} Fc_j^{L2,L3,net} \cdot P_{prd} - \sum_{pb \in PB} \sum_{i \in I} \sum_{n \in N} Fci_{pb,i,n}^{L1,L2} \cdot c_{pb} + \sum_{pbuy \in PBUY} \sum_{n \in N} F_{pbuy,n}^{buy,L2} \cdot c_{pbuy} + TC + \sum_{p \in P} SC_p + LC + DCC + MC + OMC + OC \quad (20)$$

where $Fc_j^{L2,L3,net}$ is the net flow of products prd from L2 to L3 in GWh/yr or kt/yr, P_{prd} is the price of product prd in M\$/kt or M\$/GWh, $Fci_{pb,i,n}^{L1,L2}$ is the mass flow rate of feedstocks pb from L1 to L2 in kt/yr, c_{pb} is the cost of the feedstocks pb in M\$/kt, $F_{pbuy,n}^{buy,L2}$ is the flow of the purchased materials $pbuy$ at L2 in kt/yr or GWh/yr, and c_{pbuy} is the cost of $pbuy$ in M\$/kt or M\$/GWh.

Three types of transportation ($tro \in TRO$) were assumed for the transport of raw materials and products, i.e., road transportation by truck, pipeline, and transmission lines, and were optimally selected for each material. The subset $PIPETRA$ ($PIPETRA \subset TRO$) was defined for the transportation of feedstocks or products via pipelines or power transmission lines to also take into account the investment cost. In the case of $tro \in PIPETRA$, the amount of p transported between the layers was defined as follows (Equation (21)):

$$F_{p,x,y,tro} \leq F_p^{max} \cdot y_{p,x,y,tro}, \forall p \in P, x \in \{I, N\}, y \in \{N, J\}, tro \in PIPETRA \quad (21)$$

where $F_{p,x,y,tro}$ represents the amount of p transported from i to n (L1 to L2) or n to j (L2 to L3) with the transportation option $tro \in PIPETRA$, F_p^{max} is the maximum flow, and $y_{p,x,y,tro}$ is the binary variable for the optimal selection of transportation mode (1 if the transportation mode is selected and 0 if not). The transportation costs in this case were defined using Equation (22) as the sum of the fixed and variable costs.

$$TC_{p,tro} = \sum_{x \in \{I, N\}} \sum_{y \in \{N, J\}} TC_{p,tro}^{fix} \cdot d_{x,y} \cdot y_{p,x,y,tro} + TC_{p,tro}^{var} \cdot d_{x,y} \cdot F_{p,x,y,tro}, \quad (22) \\ \forall p \in P, tro \in PIPETRA$$

Fixed transportation costs were calculated as the fixed depreciation cost $TC_{p,tro}^{fix}$ of the transmission line or pipeline per km multiplied by the length of the pipeline or transmission line ($d_{x,y}$) and binary variable $y_{p,x,y,tro}$ for the optimal selection of the transportation mode. Variable costs were further determined as the product of the variable costs $TC_{p,tro}^{var}$ in M\$/(t·km) or M\$/(GWh·km), the distance, and the amount of p transported.

In the case of road transportation ($tro \notin PIPETRA$), the transportation costs were determined using Equation (23):

$$TC_{p,tro} = \sum_{x \in \{I, N\}} \sum_{y \in \{N, J\}} TC_{p,tro}^{fix} \cdot F_{p,x,y,tro} + TC_{p,tro}^{var} \cdot d_{x,y} \cdot F_{p,x,y,tro} \cdot f_{rt}, \quad (23) \\ \forall p \in P, tro \in TRO \wedge tro \notin PIPETRA$$

where f_{rt} is the factor applied to road transportation, which was assumed to be 2 to also account for return trips.

The selection of the optimal mode of transportation for the transport of raw materials and products p between x (location i for the transport from L1 to L2 or n for the starting point from L2 to L3) and y (n in the case of L1 to L2 and j for the endpoint of the transport from L2 to L3) is obtained from Equation (24).

$$F_{p,x,y} = \sum_{tro \in TRO} F_{p,x,y,tro}, \forall x \in \{I, N\}, y \in \{N, J\}, p \in P \quad (24)$$

Finally, the total transportation costs in M\$ per year were defined as the sum of the transportation costs of feedstocks from the supply locations to the plant locations and the transportation costs of the products from the plant locations to the demand location, as shown in Equation (25).

$$TC = \sum_{pb \in PB} \sum_{tro \in TRO} TC_{pb,tro}^{L1,L2} + \sum_{prd \in PRD} \sum_{tro \in TRO} TC_{prd,tro}^{L2,L3} \quad (25)$$

Storage costs in M\$/yr were calculated using Equation (26) as the sum of the fixed and variable costs:

$$SC_p = \sum_n \sum_{stor} \left(\frac{SC_p^{fix}}{F_D} + SC_p^{var} \right) \cdot A_{n,stor,p}^{L2}, \forall p \in P \quad (26)$$

where SC_p^{fix} denotes the fixed storage costs of p in M\$ per m^2 , SC_p^{var} represents the variable storage costs in M\$/($m^2 \cdot y$), F_D is the discount factor, and $A_{n,stor,p}^{L2}$ is the area of the storage $stor$ at location n at L2. The storage area was determined as the maximum storage capacity $A_{n,stor,p}^{L2,max}$ divided by the product of the density ρ_p and height of the storage, as shown in Equation (27).

$$A_{n,stor,pb}^{L2} = \frac{A_{n,stor,p}^{L2,max}}{(\rho_p \cdot h_p^S)}, \forall n \in N, stor \in STOR, p \in P \quad (27)$$

The discount factor was determined using Equation (28) [41]:

$$F_D = \frac{(1 + r_d)^{t_D} - 1}{r_d \cdot (1 + r_d)^{t_D}} \quad (28)$$

where r_d is the discount rate, and t_D is the depreciation period.

In addition, the economic objective also considers the labor costs LC , which were determined by Equation (29):

$$LC = \sum_{n \in N} \sum_{t \in T} LC_{n,t}^{fix} \cdot y_{n,t}^{L2,T} + \sum_{n \in N} \sum_{in \in IN} \sum_{t \in T} \sum_{kp \in KP \wedge (pb,t) \in PBT \wedge (pb,prd) \in PBPRD \wedge (t,kp) \in TKP} LC_{n,t}^{var} \cdot F_{n,in,t,p}^{L2,T} \quad (29)$$

where LC in M\$/yr is the sum of the fixed ($LC_{n,t}^{fix}$) and variable ($LC_{n,t}^{var}$) labor costs due to the operation of the facilities. The fixed costs were multiplied by the binary variable to account for the existence of technology t at location n . The variable labor cost depends on the quantity of feedstocks processed, where $F_{n,in,t,p}^{L2,T}$ represents the input flow of feedstock p at site n for technology t .

Maintenance costs (MC) and other costs (OC), which include local taxes, insurance, and royalties [33], were calculated based on capital costs (CC). Usually, maintenance costs are between 5% and 15% of the installed capital cost [42]. In this study, the MC was assumed to be equal to 6% of the capital cost, as shown in Equation (30). The other costs were assumed to be 3% of the capital cost [33], as described in Equation (31).

$$MC = 0.06 \cdot CC \quad (30)$$

$$OC = 0.03 \cdot CC \quad (31)$$

Other miscellaneous costs (OMC) include laboratory expenses, supervision costs, and general overheads. Laboratory costs, which include process monitoring and quality control, are estimated to account for 20–30% of labor costs. Supervision costs account for approximately 20% of labor costs, while plant overhead costs, which include management,

security, and safety, typically account for between 50% and 100% of labor costs [42]. In this study, it was assumed that *OMC* is equal to the labor cost (Equation (32)).

$$OMC = LC \quad (32)$$

The discounted capital costs were determined using Equation (33), where the sum of the initial investments at plant locations n for technologies t ($I_{n,t}^{L2,T}$) is discounted by the discount factor F_D (Equation (28)). Further details on the determination of the *DCC* can be found in the previous work by the authors [33].

$$DCC = \frac{\sum_{n \in N} \sum_{t \in T} I_{n,t}^{L2,T}}{F_D} \quad (33)$$

2.3. Demonstration Case Study

The proposed approach of an integrated supply network and AD-HTC process flowsheet optimization was applied to the demonstration case study shown in Figure 3. Selected regions in Slovenia with a radius of 40 km and an area of 5026.5 km², which is about 25% of the total area of Slovenia, were divided into 22 zones. The zones were selected according to the availability of feedstocks and population density, which influences the demand. In each zone, the supply locations i (i_1 – i_{22}) of selected substrates are considered at L1. At L2, the potential locations of AD-HTC plants n (n_1 – n_5) and, at L3, the demand locations j (j_1 – j_{22}) are considered. The locations for the availability of feedstocks, the potential plant locations, and the demand locations with latitudes and longitudes were taken from Google Maps [43] and are shown in Part B of the Supplementary Materials. The demand locations for electricity and heat were assumed to be the largest city or town in the zone, while the potential plant locations were evenly distributed near agricultural or rural areas that were also close to cities and towns. The distances between locations (i,n), (n,j), and (n,n) were calculated using the spherical law of cosines [33]. To approximate the actual transportation distances and obtain more realistic results, a theoretical tortuosity factor (tf) of 1.27 is assumed, as proposed previously [44]. For the plants located at the same site, such as anaerobic digester, filter press, CHP, and HTC, it is assumed that the distance between them is 100 m.

The integrated supply network and the AD-HTC process flowsheet optimization problem were formulated as a MINLP model and consisted of 12,565 single equations, 23,133 continuous variables, and 2300 binary variables. The problem was formulated in the GAMS modeling interface (version 45) and solved with the DICOPT solver on a personal computer (16 GB RAM, Intel® Core™ i9-13900H processor @2.60 GHz) in a few seconds.

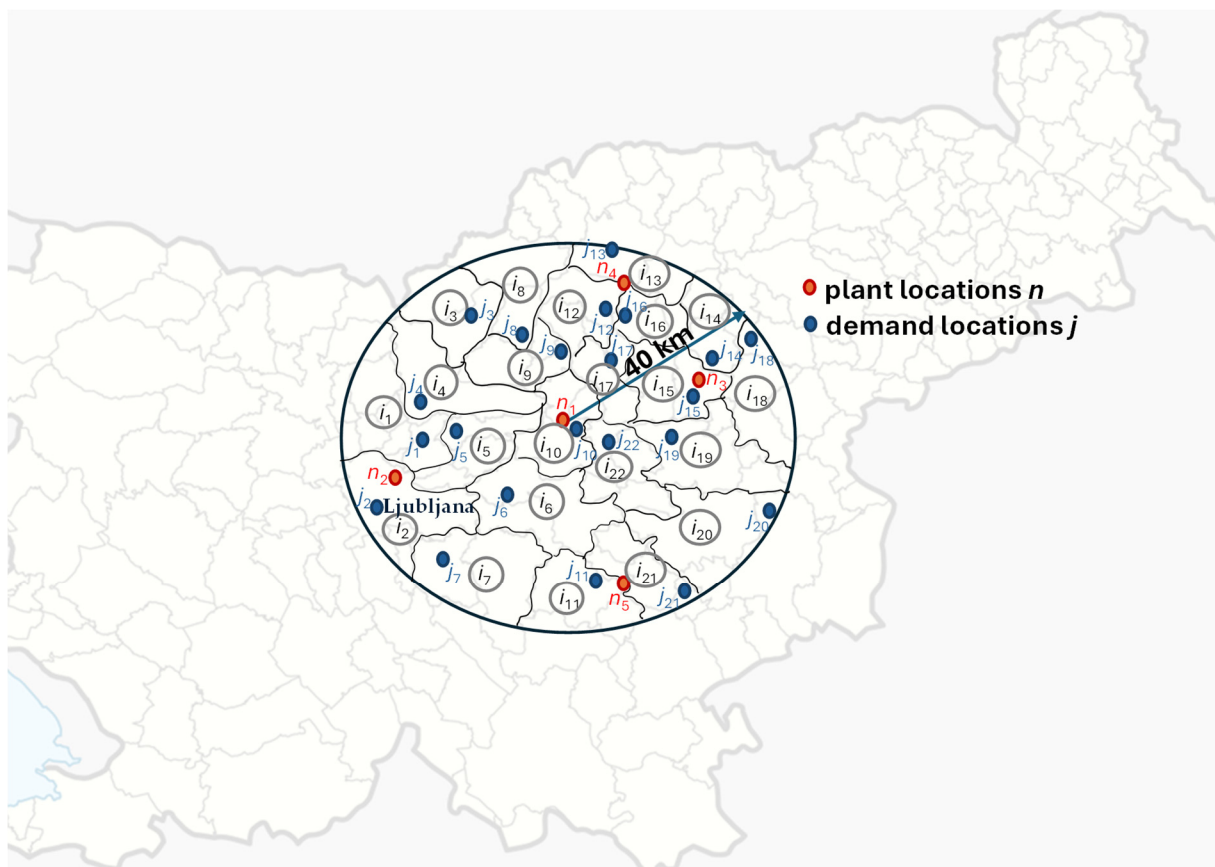


Figure 3. Demonstration case study with potential supply zones, AD-HTC plant sites, and demand locations.

3. Results and Discussion

The economic efficiency of the integrated supply chain network and the AD-HTC process was determined by considering the optimal structure of the supply chain network and the optimal AD-HTC process flow. The demand for products spr_d is a variable that is optimized according to the highest annual profit of the entire system. The main optimization results are summarized in Table 1.

The total amount of feedstocks used for AD and HTC is 1924.08 kt/yr, of which cattle manure accounts for 89.5%, as it is widely available in the selected region and has suitable characteristics for processing due to its relatively high moisture content, energy content, and methane yield. Although the selected amount of whey and sunflower cake is relatively small, it is important to use them to promote the circular bioeconomy and obtain value-added products. A total of 245.7 GWh/yr of electricity and 298.83 GWh/yr of heat was generated from five plants. It should be noted that the heat consumption within the process was also taken into account. Of the 298.83 GWh/yr of heat generated, 130.79 GWh/yr was consumed within the processes, while the remaining 168.04 GWh/yr was available for supply to the end consumers. Moreover, when losses during transportation are accounted for, only 114.45 GWh/yr of heat can be supplied to end consumers via district heating. Alternatively, the quantity of digestate and solid digestate produced from all the plants and transported to end users corresponds to 443.17 kt/yr and 1228.14 kt/yr. In addition, 185.08 kt/yr of hydrochar was produced. The revenue from the sale of all five products amounted to 91.27 M\$/yr, while the total costs amounted to 62.72 M\$/yr. The profit after taxes amounted to 23.13 M\$/yr.

Table 1. Main optimization results.

Item	Optimal Value
Feedstock (kt/yr)	
Corn silage	195.82
Cattle manure	1722.08
Sunflower cake	0.18
Whey	6.00
Total	1924.08
Products	
Electricity (GWh/yr)	245.70
Heat (GWh/yr)	298.83
Digestate (kt/yr)	443.17
Dry digestate (kt/yr)	1228.14
Hydrochar (kt/yr)	185.08
Economic results (M\$/yr)	
Revenue	91.27
Total costs	62.72
Profit before tax	28.55
Profit after tax	23.13

The optimal structure of the supply chain network is shown in Figure 4. All supply zones i (i_1 to i_{22}) were selected and the feedstocks were used in all five potential AD-HTC plants n , while seven demand locations j ($j_2, j_{10}, j_{11}, j_{12}, j_{14}, j_{18}$, and j_{22}) were selected. Selected supply zones i are marked in green, selected plant sites n in red, and the selected demand locations j in blue. Only seven (7) demand locations were optimally selected due to the transportation costs associated with the transportation of products from the plant location n to the demand location j . To reduce these costs and maximize the annual profit, all products except electricity were transported to the closest demand locations to ensure a cost-effective distribution strategy.

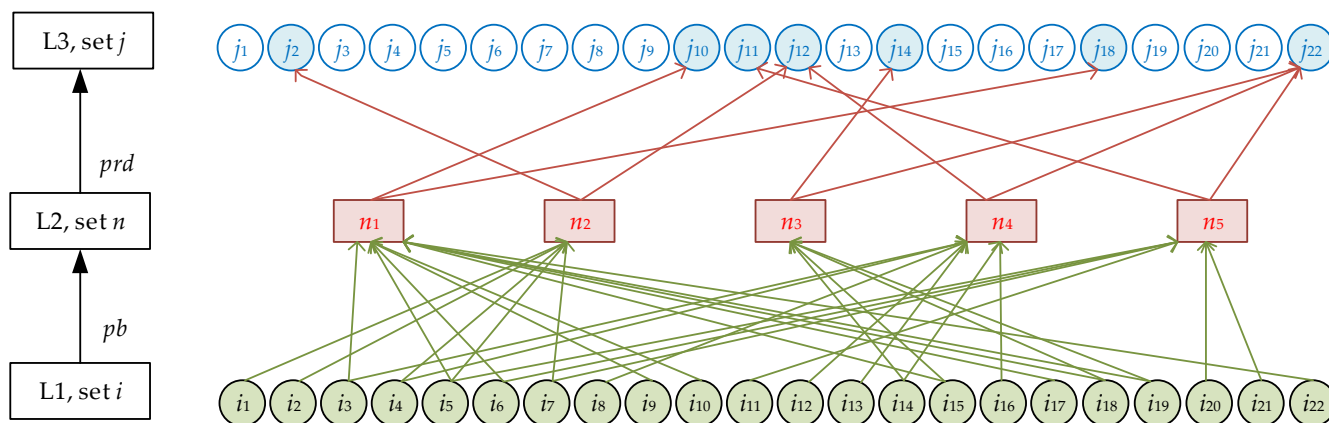


Figure 4. Optimal supply chain network structure.

Table 2 shows the amount of whey (W), corn silage (CS), sunflower cake (SC), and cattle manure (CM) selected for transportation from each supply zone i to each plant location n . It can be seen that, in 13 supply zones ($i_1, i_2, i_4, i_6, i_{10}, i_{11}, i_{12}, i_{14}, i_{15}, i_{16}, i_{17}, i_{20}$, and i_{21}), all four available feedstocks were selected and transported to the optimal (closest) plant location.

Table 2. Quantity of feedstocks pb in t/yr transported from supply zone i to plant location n .

Plant Sites/Supply Zones	n_1	n_2	n_3	n_4	n_5
i_1		W *: 326.97 CS *: 16,492.18 SC *: 10.55 CM *: 145,448.51			
i_2		W: 1123.71 CS: 15,682.97 SC: 12.02 CM: 104,898.57			
i_3	SC: 8.97			W: 211.30	
i_4		CS: 8450.63		W: 267.88 CS: 9438.51 SC: 10.75 CM: 125,034.53	
i_5	SC: 6.83	CS: 11,876.65			W: 170.20 CM: 79,439.23
i_6	CS: 10,605.01 SC: 6.08 CM: 122,940.54				W: 318.24 CS: 3508.14
i_7		SC: 12.75			W: 297.97 CS: 19,377.11
i_8				W: 234.40 SC: 4.53	
i_9	W: 103.22 CS: 7831.05 SC: 7.89				
i_{10}	W: 155.29 CS: 8826.27 SC: 4.35 CM: 94,989.79				
i_{11}					W: 229.96 CS: 10,788.72 SC: 12.62 CM: 55,375.37
i_{12}				W: 194.57 CS: 8022.06 SC: 8.08 CM: 115,525.73	
i_{13}				W: 144.01 CS: 6213.59 CM: 68,744.87	
i_{14}			W: 119.84 CS: 1155.55 CM: 93,520.83	SC: 6.54	
i_{15}	SC: 10.20		W: 800.62 CS: 10,123.07 CM: 145,782.46		
i_{16}				W: 109.52 CS: 5539.04 SC: 5.58 CM: 79,767.76	

Table 2. Cont.

Plant Sites/Supply Zones	n_1	n_2	n_3	n_4	n_5
i_{17}	W: 106.37 CS: 6207.54 SC: 6.25 CM: 89,394.91				
i_{18}	SC: 10.48		W: 164.66 CM: 149,908.38		
i_{19}	SC: 13.87		W: 254.13 CM: 198,319.17		
i_{20}					W: 324.21 CS: 19,072.60 SC: 13.87 CM: 11,750.06
i_{21}					W: 120.75 CS: 8033.96 SC: 9.39 CM: 41,235.97
i_{22}	W: 224.78 CS: 8575.81 SC: 2.29				

* W—whey, CS—corn silage, SC—sunflower cake, and CM—cattle manure.

Although all feedstocks are also available in all other zones, they were not selected, either because of the large distances to the possible plant location and the associated higher transportation costs or because of their smaller quantity, so the costs are higher than the revenue that would be obtained if they were used in the process. However, at least one feedstock was transported from each supply zone to achieve the maximum annual profit for the entire system. The optimal amount of whey and sunflower cake transported from some of the supply zones to the plants is relatively small, ranging from 2.29 t/yr to 13.87 t/yr for sunflower cake and from 103.23 t/yr to 1123.71 t/yr for whey. The reason for this is their limited availability in most supply zones. The quantity of feedstocks transported also depends on their dry matter content, as the lower and upper limits for dry matter content in the anaerobic digester and digestate were included in the model to ensure realistic and feasible operation. The largest amount of biomass was transported to plant location n_3 , with 600,149 t/yr coming from the closest supply zones (i_{14} , i_{15} , i_{18} , and i_{19}), while the smallest amount was transported to plant location n_5 (250,078 t/yr), which was the farthest from most supply zones. This result reflects the significant impact of transportation costs, as, in the optimal solution, all available raw materials were transported to the closest plant locations in order to minimize costs and maximize the profitability of the system.

Figure 5 shows the selected optimal energy and material flow from each plant site n to the end user j . For example, from plant site n_1 , the products are delivered to the demand sites j_{10} and j_{18} . Electricity is transmitted to j_{18} , while heat, solid digestate, and hydrochar are transported to j_{10} , as this location is the closest to plant location n_1 , as can also be seen in Figure 3. It should be noted that no costs have been included for the transmission of electricity, and therefore, electricity can be supplied to any demand location without affecting the costs. For other plant locations n , all the products except electricity were transported to the closest demand locations j (see also Figure 3): from n_2 to j_2 , from n_3 to j_{14} , from n_4 to j_{12} , and from n_5 to j_{11} . It was also found that only part of the digestate from plants n_2 and n_3 was selected to meet the demand. From the other plant sites, it was economically more advantageous to guide the digestate to the filter press, where the digestate with a higher dry matter content is obtained. Considering that the total amount

of solid digestate transported to the end users is almost three times higher than the amount of digestate obtained directly after AD, it can be seen that it is more worthwhile to invest money in the filter press than to sell digestate directly.

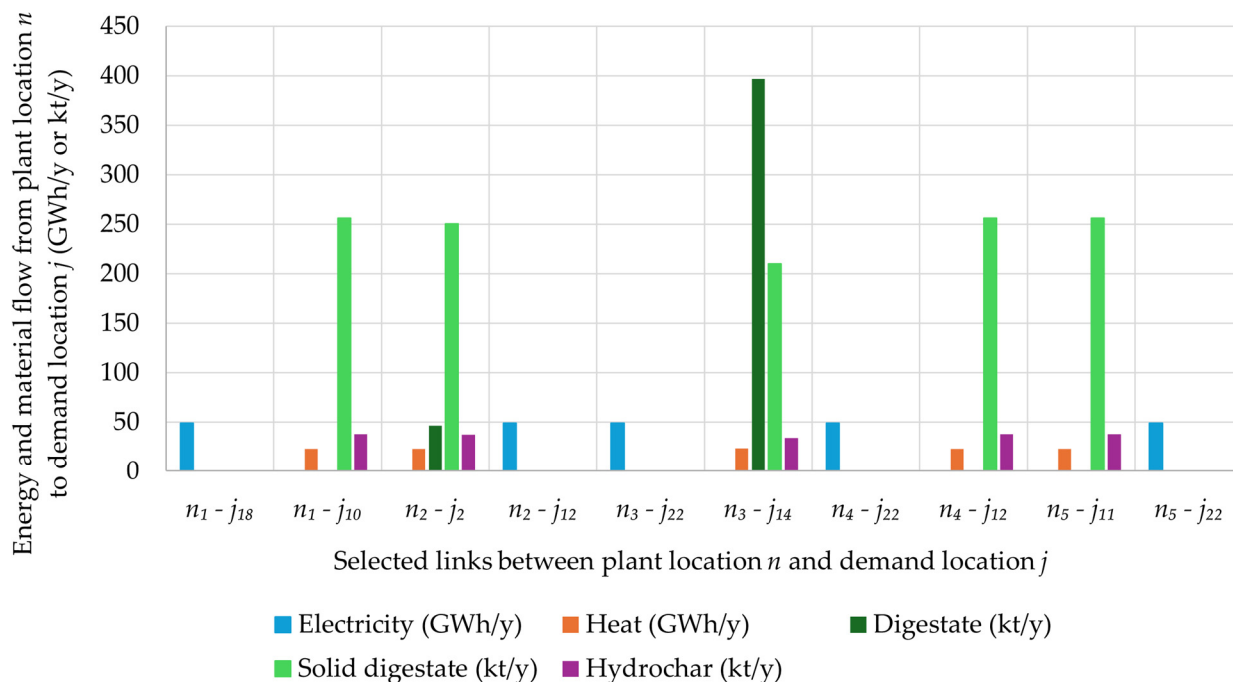


Figure 5. Optimal energy and material flow between plant location n and demand location j .

The total cost of the system includes the cost of feedstocks and purchased materials, transportation costs between the layers, storage costs, labor costs, discounted capital costs, maintenance costs, other costs, and miscellaneous costs. Figure 6 shows the breakdown of all costs incurred, with depreciation costs accounting for the largest share at 33% (20.84 M\$/yr), followed by maintenance at 17% (10.70 M\$/yr) and transport at 13% (8.02 M\$/yr). The cost of the feedstocks and storage costs account for about 11% each (6.66 M\$/yr and 6.64 M\$/yr), while the remaining costs (other costs, miscellaneous costs, labor costs, and costs of purchased materials) account for 15% in total.

The costs for the transportation of raw materials amounted to 3.28 M\$/yr and, for the products, to 4.74 M\$/yr, of which 3.23 M\$/yr was attributable to heat distribution by the pipeline, as the construction of a new pipelines was taken into account. Road transportation was considered for the transportation of solid digestate and hydrochar, while transmission lines were assumed for the distribution of electricity. For the transportation of feedstocks from i to n , only road transportation was chosen. In the superstructure, the option of transportation via pipeline was also considered for whey and cow manure, but due to the higher fixed costs associated with the construction of a pipeline, this was not chosen. Two options were also considered for the transportation of the digestate, namely pipeline and road transport, with road transport also being chosen.

To determine when the transportation of cattle manure and digestate by pipeline is more cost-effective than transportation by road, we conducted a sensitivity analysis comparing the transportation costs of both modes of transport as a function of distance. The analysis was performed for a representative amount of each feedstock, namely 145.45 kt/yr of cattle manure (the amount transported from i_1 to n_2) and 46.62 kt/yr of digestate (the amount transported from n_2 to j_2). The costs were calculated for different transportation distances, taking into account the fixed and variable cost components for both pipeline and road transportation. Figure 7 illustrates the results of this analysis and shows the

comparison of transportation costs for the pipeline and road transport as a function of distance for (a) cattle manure and (b) digestate. It was found that the pipeline is the optimal mode of transportation for cattle manure for distances of less than 2.85 km and, for digestate, for the distances of less than 4.00 km. Since the distances between *i* and *n* were greater than 6.33 km for all possible routes in our case study, road transportation was selected as the optimal option for the transportation of cattle manure. For digestate, the distances between all possible routes between *n* and *j* were also greater than 6.25 km, so road transportation was also selected as the optimal transportation option.

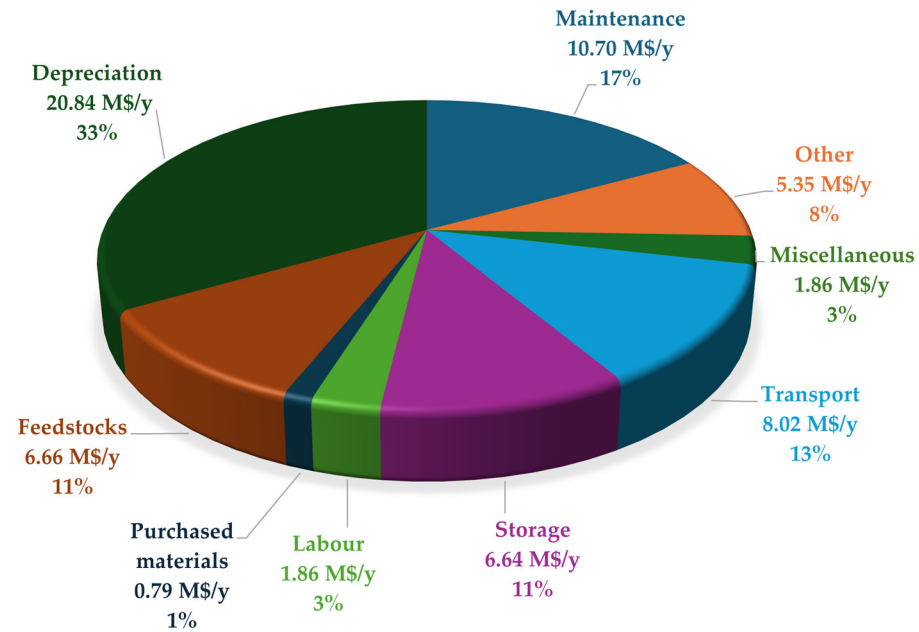


Figure 6. Cost breakdown.

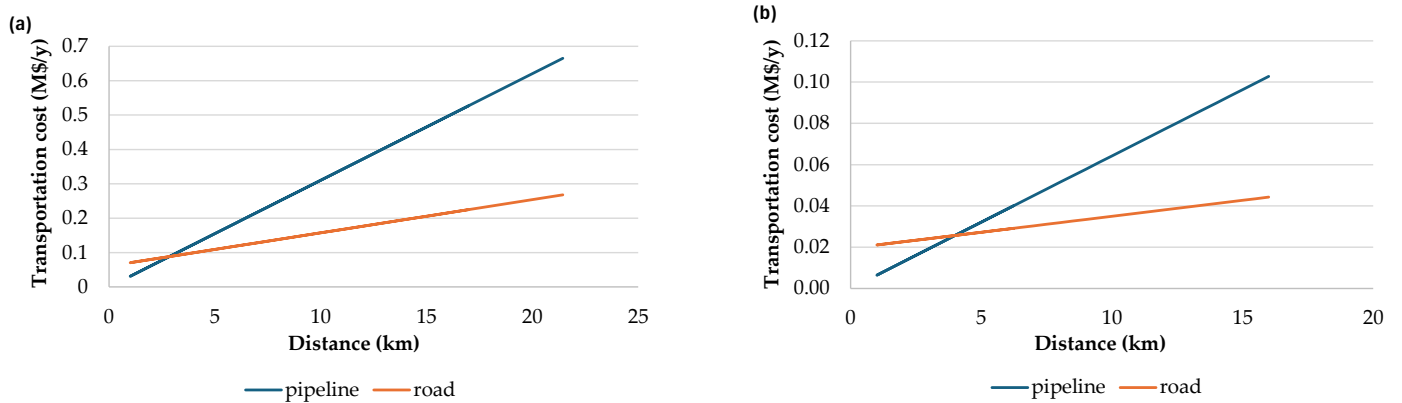


Figure 7. Comparison of the transportation costs for road and pipeline transport of (a) cattle manure and (b) digestate.

Figure 8 shows the income distribution of the products supplied by all five plants to the demand locations. The sales prices assumed in the model are 0.155 M\$/GWh for electricity [45], 0.077 M\$/GWh for heat [46], 4.86 \$/t for digestate [47], 11.77 \$/t for solid digestate [48], and 150 \$/t for hydrochar [49]. The electricity price was determined based on the average monthly day ahead trading prices from the Slovenian auction market. The results show that electricity is the largest source of revenue at 42% (38.08 M\$/yr), followed by hydrochar at 30% (27.76 M\$/yr), highlighting the benefits of electricity generation and the production of hydrochar that can be used as a biofuel, soil conditioner, etc. Solid digestate provides 16% (14.46 M\$/yr), highlighting its potential for use as a soil conditioner

or in agriculture, while heat contributes 10% (8.81 M\$/yr). Wet digestate only accounts for 2% (2.15 M\$/yr) due to its relatively low market value, which could be increased in the case of dewatering. The results also show that it is important to include cogeneration in the overall process flowsheet, as electricity and heat account for 52% of the total revenue. However, it should be noted that the production of other alternatives from biogas, such as pure methane or hydrogen, are not considered in this study.

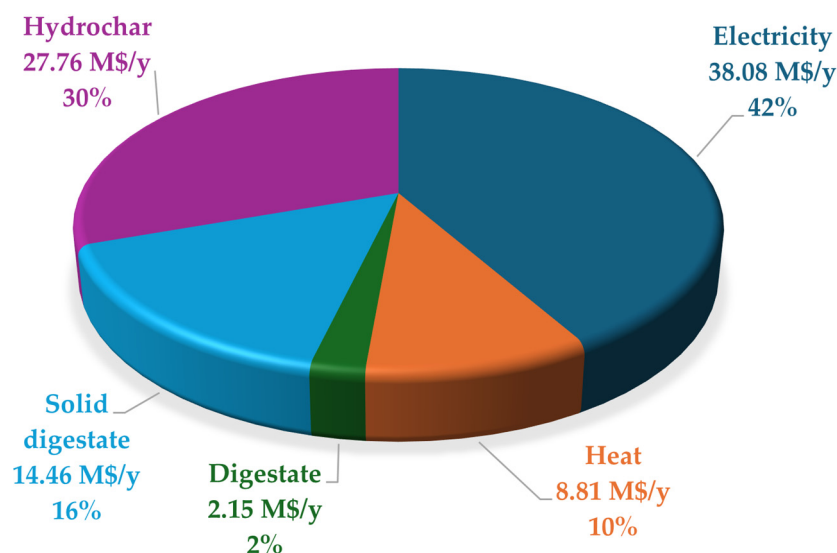


Figure 8. Income from various products.

Simultaneously with the optimal structure of the supply network, the optimal process design was also determined. Figure 9 shows the optimum process flowsheet for the plant at location n_1 . It can be observed that the MXR-1 unit contains 1386 kt/yr of substrates with a dry matter content of 10.73%. In the splitter, this stream is then separated, and the optimal solution shows that 90% of the substrate goes to AD, while the remaining 10% goes to MXR-2 and, subsequently, to HTC. The digestate obtained from AD (approx. 1219 kt/yr) with a dry matter content of 8.62% is then transported to PRESS, while no digestate goes directly to the demand locations. From PRESS, solid and liquid fractions are obtained. The solid fraction is partly used as a substrate for the HTC, and partly, it is transported to the demand points. The liquid fraction is sent back to the MXR-1 unit and reused as a substrate for the AD and HTC processes. PRESS produces 366 kt/yr of the solid fraction with a dry matter content of 25% and 853 kt/yr of the liquid fraction with a solid content of 1.6. The solid fraction is then mainly (70%) transported to the end users (256 kt/yr) and partly (30%) to MXR-2 and then to HTC. The total amount of substrates available for the HTC is 248 kt/yr and contains 17.04% of dry matter.

The products of the HTC are the water phase, namely 197 kt/yr, the gas phase, which accounts for 3.34% of the total flow into the HTC, and 38 kt/yr of hydrochar with 80% dry matter content. The heat requirements are covered by heat generation in a CHP plant. The biogas obtained from the AD is utilized within a gas engine (CHP plant), where 49.14 GWh/yr of electricity and 59.77 GWh/yr of heat are generated. Of this, 26.16 GWh/yr of heat is used to cover the heat demand within the entire plant, while 33.61 GWh/yr remains available for distribution to the demand locations. Accounting for the losses due to transport to the end consumers, 22.76 GWh/yr of heat was distributed from the plant n_1 to the demand location j_{10} , which is the shortest distance away (8.04 km).

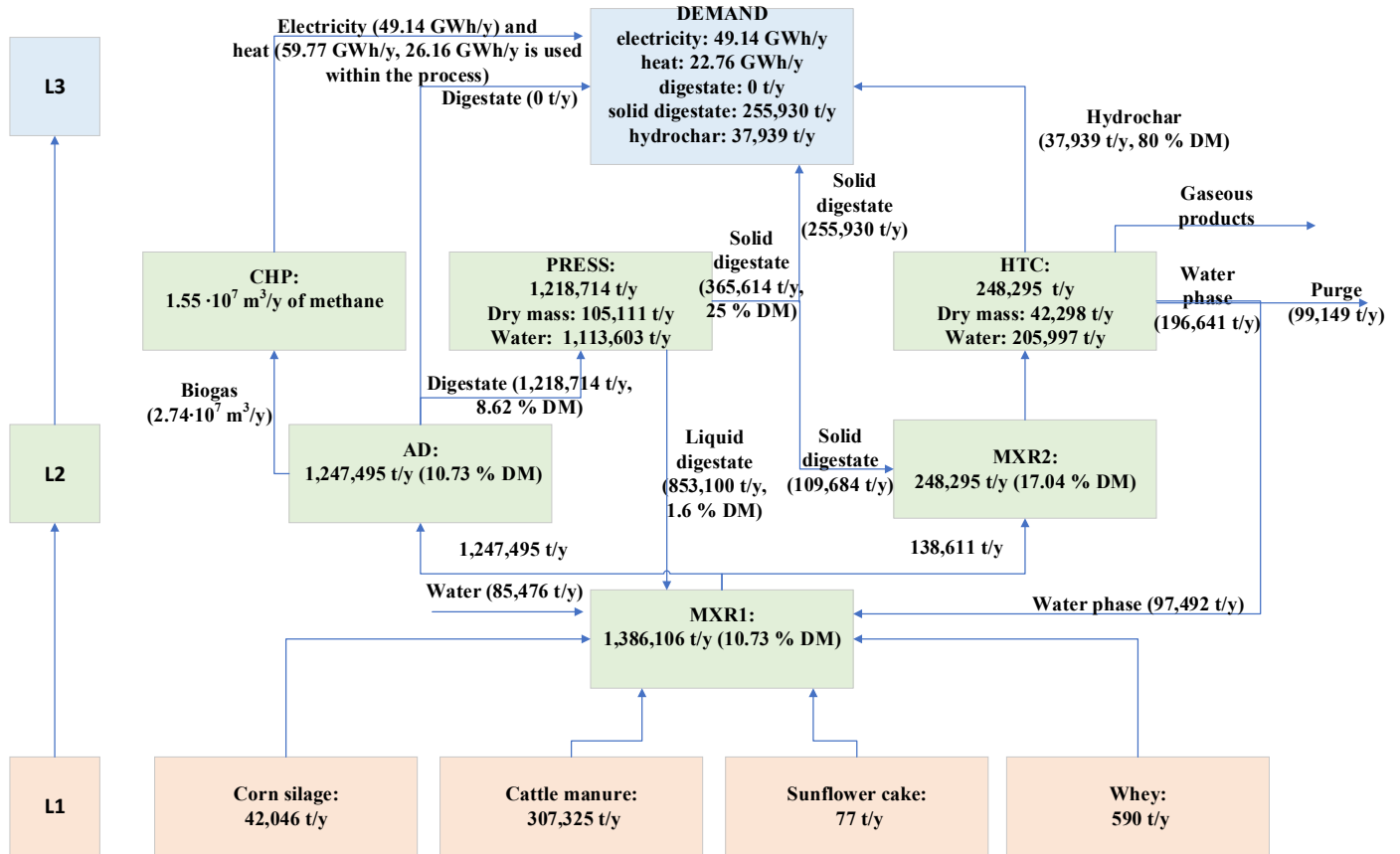


Figure 9. Optimal process flowsheet for the AD-HTC plant at location n_1 .

4. Conclusions

The study presented a comprehensive approach and methodology for the simultaneous optimization of the biomass supply chain network and process flowsheet, which includes anaerobic digestion, cogeneration, and hydrothermal carbonization. The integration of AD and HTC processes is essential for improving energy recovery from biomass. However, holistic system optimization also requires an efficient supply chain, which minimizes transportation routes and reduces costs while ensuring a reliable feedstock flow and strategically optimizing resource utilization to improve the overall sustainability. The proposed MINLP model was applied to the demonstration case study, which considers a region in the shape of a circle in Slovenia.

The optimal design of the supply network, with the locations of the supply zones, plants, and end users and selected transportation modes and routes, is presented together with the optimal values for the process variables to achieve the maximum efficiency and economic performance of the whole system. The results show that biomass utilization by AD and HTC is economically viable, with an annual profit of 23.13 M\$/yr, with electricity, hydrochar, and heat accounting for 42%, 30%, and 10% of the total revenue, respectively. Discounted capital costs account for the largest share of annual costs at 33%, followed by maintenance at 17% and transportation at 13%. As different transportation modes were considered for some of the feedstocks and products (cattle manure, whey, and digestate), a sensitivity analysis was carried out, and the breakeven point at which pipelines become more cost-efficient than road transport was determined.

These results demonstrate the practical applicability of the proposed approach in real-world scenarios and provide actionable insights for optimizing supply chain logistics and process configurations. The model could support industries and policymakers in improving resource efficiency and sustainability. Its adaptability to other regions or systems with

similar feedstocks and logistical challenges makes it a scalable and flexible solution for bioresource management.

Future research could incorporate environmental and social perspectives through a composite sustainability criterion, including indicators such as greenhouse gas emissions, land use, water scarcity, new job creation, etc., to enable a sustainability assessment of the system. Additionally, the model could be extended to a multi-period optimization to account for dynamic changes in prices and resource availability and to analyze the contents of carbon, nitrogen, phosphorus, heavy metals, and other substances in digestate and hydrochar.

Supplementary Materials: The following supporting information can be downloaded at <https://www.mdpi.com/article/10.3390/en18020334/s1>: Table S1: Dry matter content of the feedstocks; Table S2: Biogas yields from different substrates; Table S3: Methane content in biogas from different substrates; Table S4: Conversion factors for CHP; Table S5: Data for estimating the capital costs of technologies; Table S6: Fixed and variable transportation costs of feedstocks and products; Table S7: Costs of feedstocks; Table S8: Selling prices for products; Table S9: Latitudes and longitudes of the edge and center of the supply zones i at L1 and the total area of each zone; Table S10: Latitudes and longitudes of the demand locations j at L3; Table S11: Latitudes and longitudes of the plant locations n at L2. References [50–53] are cited in the Supplementary Materials.

Author Contributions: Conceptualization, S.P., A.P. and L.Č.; methodology, S.P., L.Č. and J.M.E.; software, L.Č. and S.P.; validation, S.P., L.Č. and J.M.E.; investigation, S.P., A.P., J.M.E. and L.Č.; data curation, S.P. and J.M.E.; writing—original draft preparation, S.P.; writing—review and editing, L.Č., J.M.E. and A.P.; visualization, S.P.; supervision, L.Č. All authors have read and agreed to the published version of the manuscript.

Funding: This research was funded by the Slovenian Research and Innovation Agency (Research Core Fundings Nos. P2-0414 and P2-0421 and projects Nos. J4-50149 and N2-0361).

Data Availability Statement: The original contributions presented in this study are included in the article/Supplementary Materials. Further inquiries can be directed to the corresponding author.

Conflicts of Interest: The authors declare no conflicts of interest.

References

1. Oumabady, S.; Ramasamy, S.P.; Paul Sebastian, S.; Rajagopal, R.; Obulisamy, P.K.; Doherty, R.; Nanukuttan, S.; Bhardwaj, S.K.; Kumaresan, D. Sustainable resource recovery and process improvement in anaerobic digesters using hydrochar: A circular bio-economic perspective. *J. Sustain. Agric. Environ.* **2023**, *2*, 328–336. [[CrossRef](#)]
2. Zeymer, M.; Meisel, K.; Clemens, A.; Klemm, M. Technical, economic, and environmental assessment of the hydrothermal carbonization of green waste. *Chem. Eng. Technol.* **2017**, *40*, 260–269. [[CrossRef](#)]
3. Reza, M.T.; Andert, J.; Wirth, B.; Busch, D.; Pielert, J.; Lynam, J.G.; Mumme, J. Hydrothermal carbonization of biomass for energy and crop production. *Appl. Bioenergy* **2014**, *1*, 11–29. [[CrossRef](#)]
4. Sarker, S.; Lamb, J.J.; Hjelme, D.R.; Lien, K.M. A review of the role of critical parameters in the design and operation of biogas production plants. *Appl. Sci.* **2019**, *9*, 1915. [[CrossRef](#)]
5. Inayat, A.; Ahmed, S.F.; Djamanroodi, F.; Al-Ali, F.; Alsallani, M.; Mangoosh, S. Process simulation and optimization of anaerobic Co-digestion. *Front. Energy Res.* **2021**, *9*, 764463. [[CrossRef](#)]
6. Tabatabaei, M.; Valijanian, E.; Aghbashlo, M.; Ghanavati, H.; Sulaiman, A.; Wakisaka, M. Prominent parameters in biogas production systems. *Biogas Fundam. Process Oper.* **2018**, *6*, 135–161.
7. Pauline, A.L.; Joseph, K. Hydrothermal carbonization of organic wastes to carbonaceous solid fuel—A review of mechanisms and process parameters. *Fuel* **2020**, *279*, 118472. [[CrossRef](#)]
8. Zhuang, X.; Liu, J.; Zhang, Q.; Wang, C.; Zhan, H.; Ma, L. A review on the utilization of industrial biowaste via hydrothermal carbonization. *Renew. Sustain. Energy Rev.* **2022**, *154*, 111877. [[CrossRef](#)]
9. Zhou, Y.; Engler, N.; Nelles, M. Symbiotic relationship between hydrothermal carbonization technology and anaerobic digestion for food waste in China. *Bioresour. Technol.* **2018**, *260*, 404–412. [[CrossRef](#)]

10. Kosińska, N.; Krzyżyńska, R.; Ghazal, H.; Jouhara, H. Hydrothermal carbonisation of sewage sludge and resulting biofuels as a sustainable energy source. *Energy* **2023**, *275*, 127337. [[CrossRef](#)]
11. Ipiates, R.; de La Rubia, M.; Diaz, E.; Mohedano, A.; Rodriguez, J.J. Integration of hydrothermal carbonization and anaerobic digestion for energy recovery of biomass waste: An overview. *Energy Fuels* **2021**, *35*, 17032–17050. [[CrossRef](#)]
12. Czerwińska, K.; Śliz, M.; Wilk, M. Hydrothermal carbonization process: Fundamentals, main parameter characteristics and possible applications including an effective method of SARS-CoV-2 mitigation in sewage sludge. A review. *Renew. Sustain. Energy Rev.* **2022**, *154*, 111873. [[CrossRef](#)]
13. Cavali, M.; Junior, N.L.; de Almeida Mohedano, R.; Belli Filho, P.; da Costa, R.H.R.; de Castilhos Junior, A.B. Biochar and hydrochar in the context of anaerobic digestion for a circular approach: An overview. *Sci. Total Environ.* **2022**, *822*, 153614. [[CrossRef](#)]
14. Wang, X.; Zhao, J.; Yang, Q.; Sun, J.; Peng, C.; Chen, F.; Xu, Q.; Wang, S.; Wang, D.; Li, X.; et al. Evaluating the potential impact of hydrochar on the production of short-chain fatty acid from sludge anaerobic digestion. *Bioresour. Technol.* **2017**, *246*, 234–241. [[CrossRef](#)]
15. Yang, Y.; Wang, M.; Yan, S.; Yong, X.; Zhang, X.; Awasthi, M.K.; Xi, Y.; Zhou, J. Effects of hydrochar and biogas slurry reflux on methane production by mixed anaerobic digestion of cow manure and corn straw. *Chemosphere* **2023**, *310*, 136876. [[CrossRef](#)]
16. Pawlak-Kruczek, H.; Niedzwiecki, L.; Sieradzka, M.; Mlonka-Mędrała, A.; Baranowski, M.; Serafin-Tkaczuk, M.; Magdziarz, A. Hydrothermal carbonization of agricultural and municipal solid waste digestates—Structure and energetic properties of the solid products. *Fuel* **2020**, *275*, 117837. [[CrossRef](#)]
17. Appala, V.N.S.G.; Pandhare, N.N.; Bajpai, S. Mathematical models for optimization of anaerobic digestion and biogas production. In *Zero Waste Biorefinery*; Springer: Berlin/Heidelberg, Germany, 2022; pp. 575–591.
18. Ramachandran, A.; Rustum, R.; Adeloje, A.J. Review of anaerobic digestion modeling and optimization using nature-inspired techniques. *Processes* **2019**, *7*, 953. [[CrossRef](#)]
19. Ali, A.; Keerio, H.A.; Abro, O.A.; Noor, M.; Panhwar, S.; Mahar, R.B. A Study of Mathematical Models Used in Anaerobic Digestion of Organic Refuse. *VFAST Trans. Math.* **2024**, *12*, 150–163. [[CrossRef](#)]
20. Al-Rubaye, H.; Karambelkar, S.; Shivashankaraiah, M.M.; Smith, J.D. Process simulation of two-stage anaerobic digestion for methane production. *Biofuels* **2019**, *10*, 181–191. [[CrossRef](#)]
21. Rajendran, K.; Kankanala, H.R.; Lundin, M.; Taherzadeh, M.J. A novel process simulation model (PSM) for anaerobic digestion using Aspen Plus. *Bioresour. Technol.* **2014**, *168*, 7–13. [[CrossRef](#)] [[PubMed](#)]
22. Harun, N.; Othman, N.; Zaki, N.; Rasul, N.M.; Samah, R.; Hashim, H. Simulation of anaerobic digestion for biogas production from food waste using SuperPro designer. *Mater. Today Proc.* **2019**, *19*, 1315–1320. [[CrossRef](#)]
23. Nazos, A.; Politi, D.; Giakoumakis, G.; Sidoras, D. Simulation and optimization of lignocellulosic biomass wet-and dry-torrefaction process for energy, fuels and materials production: A review. *Energies* **2022**, *15*, 9083. [[CrossRef](#)]
24. Ischia, G.; Fiori, L. Hydrothermal carbonization of organic waste and biomass: A review on process, reactor, and plant modeling. *Waste Biomass Valorization* **2021**, *12*, 2797–2824. [[CrossRef](#)]
25. Ubene, M.; Heidari, M.; Dutta, A. Computational modeling approaches of hydrothermal carbonization: A critical review. *Energies* **2022**, *15*, 2209. [[CrossRef](#)]
26. Gómez, J.; Corsi, G.; Pino-Cortés, E.; Díaz-Robles, L.A.; Campos, V.; Cubillos, F.; Pelz, S.K.; Paczkowski, S.; Carrasco, S.; Silva, J. Modeling and simulation of a continuous biomass hydrothermal carbonization process. *Chem. Eng. Commun.* **2020**, *207*, 751–768. [[CrossRef](#)]
27. Moser, L.; Penke, C.; Batteiger, V. An in-depth process model for fuel production via hydrothermal liquefaction and catalytic hydrotreating. *Processes* **2021**, *9*, 1172. [[CrossRef](#)]
28. Hao, B.; Xu, D.; Wei, Y.; Diao, Y.; Yang, L.; Fan, L.; Guo, Y. Mathematical models application in optimization of hydrothermal liquefaction of biomass. *Fuel Process. Technol.* **2023**, *243*, 107673. [[CrossRef](#)]
29. Aragón-Briceño, C.; Ross, A.; Camargo-Valero, M. Mass and energy integration study of hydrothermal carbonization with anaerobic digestion of sewage sludge. *Renew. Energy* **2021**, *167*, 473–483. [[CrossRef](#)]
30. Wang, R.; Lin, K.; Peng, P.; Lin, Z.; Zhao, Z.; Yin, Q.; Ge, L. Energy yield optimization of co-hydrothermal carbonization of sewage sludge and pinewood sawdust coupled with anaerobic digestion of the wastewater byproduct. *Fuel* **2022**, *326*, 125025. [[CrossRef](#)]
31. Medina-Martos, E.; Istrate, I.-R.; Villamil, J.A.; Gálvez-Martos, J.-L.; Dufour, J.; Mohedano, Á.F. Techno-economic and life cycle assessment of an integrated hydrothermal carbonization system for sewage sludge. *J. Clean. Prod.* **2020**, *277*, 122930. [[CrossRef](#)]
32. Nunes, L.; Causer, T.; Ciolkosz, D. Biomass for energy: A review on supply chain management models. *Renew. Sustain. Energy Rev.* **2020**, *120*, 109658. [[CrossRef](#)]
33. Egieya, J.M.; Čuček, L.; Zirngast, K.; Isafiade, A.J.; Pahor, B.; Kravanja, Z. Synthesis of biogas supply networks using various biomass and manure types. *Comput. Chem. Eng.* **2019**, *122*, 129–151. [[CrossRef](#)]
34. Searcy, E.; Flynn, P.; Ghafoori, E.; Kumar, A. The relative cost of biomass energy transport. *Appl. Biochem. Biotechnol.* **2007**, *137*, 639–652. [[PubMed](#)]

35. Statistical Office of the Republic of Slovenia. Available online: <https://pxweb.stat.si/SiStatData/pxweb/en/Data/Data/15P2101S.px/> (accessed on 22 June 2024).
36. Statistical Office of the Republic of Slovenia. Available online: <https://pxweb.stat.si/SiStatData/pxweb/en/Data/Data/1502410S.px/> (accessed on 23 June 2024).
37. Statistical Office of the Republic of Slovenia. Available online: <https://pxweb.stat.si/SiStatData/pxweb/en/Data/Data/1573804S.px/> (accessed on 23 June 2024).
38. Statistical Office of the Republic of Slovenia. Available online: <https://pxweb.stat.si/SiStatData/pxweb/en/Data/Data/1514504S.px/> (accessed on 24 June 2024).
39. Nowak, M.; Czekala, W. Sustainable Use of Digestate from Biogas Plants: Separation of Raw Digestate and Liquid Fraction Processing. *Sustainability* **2024**, *16*, 5461. [CrossRef]
40. Zaccariello, L.; Battaglia, D.; Morrone, B.; Mastellone, M. Hydrothermal carbonization: A pilot-scale reactor design for bio-waste and sludge pre-treatment. *Waste Biomass Valorization* **2022**, *13*, 3865–3876. [CrossRef]
41. Drobež, R.; Novak Pintarič, Z.; Pahor, B.; Kravanja, Z. Simultaneous heat integration and the synthesis of biogas processes from animal waste. *Asia-Pac. J. Chem. Eng.* **2011**, *6*, 734–749. [CrossRef]
42. Sinnott, R. *Chemical Engineering Design. Coulson Richardson's Chemical Engineering*, 4th ed.; Elsevier: Amsterdam, The Netherlands, 2005; Volume 6.
43. Google Maps. Available online: <https://maps.google.com> (accessed on 6 June 2024).
44. Sultana, A.; Kumar, A. Development of tortuosity factor for assessment of lignocellulosic biomass delivery cost to a biorefinery. *Appl. Energy* **2014**, *119*, 288–295. [CrossRef]
45. BSP Energy Exchange LLC. Available online: <https://www.bsp-southpool.com/day-ahead-trading-results-si.html> (accessed on 14 August 2024).
46. Energetika Ljubljana. Available online: <https://www.energetika.si/ceniki/cenik-plin> (accessed on 14 August 2024).
47. Lamolinara, B.; Pérez-Martínez, A.; Guardado-Yordi, E.; Fiallos, C.G.; Diéguez-Santana, K.; Ruiz-Mercado, G.J. Anaerobic digestate management, environmental impacts, and techno-economic challenges. *Waste Manag.* **2022**, *140*, 14–30. [CrossRef]
48. Jurgutis, L.; Šlepetienė, A.; Šlepetys, J.; Cesevičienė, J. Towards a full circular economy in biogas plants: Sustainable management of digestate for growing biomass feedstocks and use as biofertilizer. *Energies* **2021**, *14*, 4272. [CrossRef]
49. Saba, A.; McGaughy, K.; Reza, M.T. Techno-economic assessment of co-hydrothermal carbonization of a coal-Miscanthus blend. *Energies* **2019**, *12*, 630. [CrossRef]
50. Kucher, O.; Hutsol, T.; Glowacki, S.; Andreitseva, I.; Dibrova, A.; Muzychenko, A.; Szeląg-Sikora, A.; Szparaga, A.; Kocira, S. Energy potential of biogas production in Ukraine. *Energies* **2022**, *15*, 1710. [CrossRef]
51. The Engineering ToolBox. Fuels—Higher and Lower Calorific Values. Available online: https://www.engineeringtoolbox.com/fuels-higher-calorific-values-d_169.html (accessed on 22 July 2024).
52. Akbari, M.; Oyedun, A.O.; Kumar, A. Comparative energy and techno-economic analyses of two different configurations for hydrothermal carbonization of yard waste. *Bioresour. Technol. Rep.* **2019**, *7*, 100210. [CrossRef]
53. MARIBORSKI VODOVOD, javno podjetje., d.o.o. Available online: <https://www.mb-vodovod.si/uporabniki/obracun-vode/obracun-in-cena-pitne-vode/cenik-vode/> (accessed on 12 July 2024).

Disclaimer/Publisher's Note: The statements, opinions and data contained in all publications are solely those of the individual author(s) and contributor(s) and not of MDPI and/or the editor(s). MDPI and/or the editor(s) disclaim responsibility for any injury to people or property resulting from any ideas, methods, instructions or products referred to in the content.